BNL-62682

CONF-9609104--1

TEXTURE DETERMINATIONS IN RARE-EARTH-BASED PERMANENT MAGNETS

L. H. LEWIS
D. O. WELCH
Materials Science Division, Department of Applied Science,
Brookhaven National Laboratory
Upton, New York 11973-5000, U.S.A.

T. R. THURSTON
Department of Physics
Brookhaven National Laboratory
Upton, New York 11973-5000, U.S.A.

and

V. PANCHANATHAN
Magnequench International, Inc.
6435 Scatterfield Road
Anderson, Indiana 46013, U.S.A.

ABSTRACT

Quantifying the relationship between crystallographic texture and magnetic properties is highly desirable for the engineering high $(BH)_{max}$ magnets. Existing techniques for the evaluation of texture in permanent magnets often rely upon magnetic remanence measurements. However, such determinations are strictly applicable only to assemblies of non-interacting particles, which nullifies the use of the Stoner-Wohlfarth criteria in texture determinations of "exchange-spring" magnets. New techniques in the determination of texture of bulk permanent magnets are being developed to overcome these inherent experimental difficulties. Crystallographic alignment studied by transmission synchrotron x-ray diffraction as a function of position within the sample reveals insights into the development of texture with deformation level in thermomechanically-processed magnets. Information concerning texture may also be obtained by a different method based on paramagnetic susceptibility measurements. Such measurements also provide Curie temperature data, which is sensitive to chemical changes that may have occurred in the magnetic phase during processing.

1. Introduction

High remanence B_r produced by maximal crystallographic alignment of constituent grains is arguably the most effective extrinsic parameter for the attainment of large energy

products $(BH)_{max}$ in rare-earth-based permanent magnets such as $Nd_2Fe_{14}B$. Continued improvements in processing to obtain a high degree of crystallographic texture are essential for the engineering of increasingly higher $(BH)_{max}$ magnets.

Unfortunately, the degree of crystallographic alignment in bulk magnets is not a trivial parameter to determine. A number of methods based on a variety of measurements using magnetic[1], diffraction[2] and microscopy techniques (electron[3] and optical[4]) exist to evaluate texture, but limitations of each technique exist and must be evaluated for their applicability before application to bulk magnet systems. By way of example, the anticipated emergence of two-phase anisotropic "exchange-spring" magnets consisting of a magnetically soft phase intimately mixed with an aligned hard phase[5] presents significant challenges in the determination of the degree of orientation of the ensemble of crystallites of the hard phase. In this case the essential exchange interactions amongst the constituent phases nullify the use of techniques that utilize measurements of the remanence B_r, such as the angular dependence of B_r[6] or the remanence ratio B_r/M_s[7].

Novel techniques in the determination of crystallographic orientation of bulk permanent magnets are being developed to overcome challenges inherent to advanced permanent magnets. We describe here two previously-unexplored independent methods that may be used to evaluate texture in bulk magnets: Transmission synchrotron x-ray diffraction and paramagnetic susceptibility measurements.

Transmission synchrotron x-ray diffraction may be used to probe crystallographic texture in a significant volume of material, providing a quasi-bulk determination of texture. Transmission x-ray diffraction is advantageous over conventional laboratory reflection x-ray diffraction in that the resultant data are insensitive to the condition of the specimen's surface. We apply the technique of transmission x-ray diffraction to generate rocking curves of the basal (006) reflection as a function of position within 2-14-1 magnets that have been melt-quenched and thermomechanically deformed (MQ-3) to varying degrees. The width of the rocking curve provides a measure of the angular deviation from ideal axial orientation of the probed volume fraction of the magnet's crystallites.

Information concerning crystallographic texture may also be obtained by analysis of the temperature dependence of the inverse paramagnetic susceptibility. The data must be taken at elevated temperatures, at least 50 K above the ferromagnetic Curie temperature of the phase of interest. This method also allows an examination of the samples' paramagnetic Curie temperatures, allowing one to easily monitor any chemical changes that may have occurred in the paramagnetic phase during processing steps.

2. Novel Experimental Methods to Determine Texture

2.1. Transmission Synchrotron X-ray Diffraction Studies

Transmission x-ray diffraction experiments were performed on Beamline X27-A at the National Synchrotron Light Source on a series of $RE_2Fe_{14}B$-based samples that had been subjected to various degrees of thermomechanical deformation.

Samples with the nominal composition $Nd_{2.43}(Fe_{0.92}Co_{0.08})_{14}B_{0.92}Ga_{0.09}$ were made from ribbons of melt-quenched precursors that were consolidated and then hot-pressed to obtain close to 100% theoretical density. The hot-pressed samples were then placed in cylindrical oversized dies and heated to 800°C while under a uniaxial pressure of approximately 5.5 GPa for various amounts of time to produce samples with different lev-

els of deformation. The degree of deformation, or die-upset (DU), is defined by subtracting the ratio of the final height to the initial height from unity. In this paper the results obtained from samples with 0% DU, 42% DU and 70% DU will be examined. Fig. 1 shows room-temperature hysteresisgraph demagnetization curves taken after subjecting the samp-

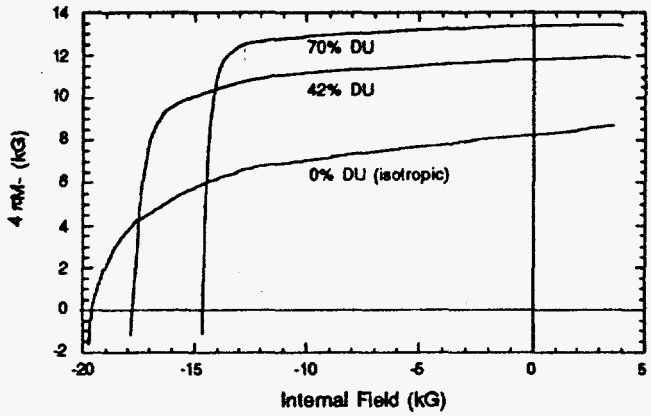

Figure 1. Second-quadrant demagnetization curves for melt-quenched samples of various deformation levels.

les to an axial premagnetizing pulsed field of 4 T. All deformed samples show a high remanence and a good squareness; an increased level of deformation is always accompanied by a decrease in the coercivity and an increase in the remanence. After the bulk magnetic measurements were performed, x-ray measurements were made on a thin slice of thickness $\approx 0.4mm$ which was cut parallel to the press direction from the measured geometric center of each sample with a slow-speed wire saw. The slice incorporates the entire diameter of the magnet; no surface preparation of the sample other than cleaning was performed. The geometry of the transmission x-ray diffraction set up is illustrated in Fig. 2; k_i and k_f are the initial and final x-ray momentum vectors, respectively. In this geometry the entire sample volume is probed, rather than the $\approx 1\mu m$ depth near the surface that is probed in the reflection geometry. A Si (111) crystal was used to produce a monochromatic x-ray

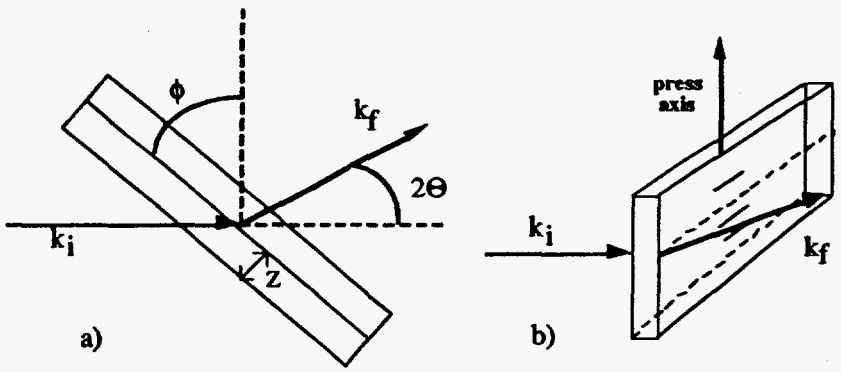

Figure 2. a). Transmission x-ray diffraction geometry; b). Schematic diagram of horizontal and vertical raster scans.

beam with an energy of approximately 25.5 keV, which corresponds to a wavelength λ = 0.5048 Å. The area of the beam incident upon the sample was ~ 1*mm* x 5*mm*. The samples were attached to a holder using adhesive tape, and all measurements were performed at room temperature. 2Θ scans were first done in the center of each sample in geometries parallel and perpendicular to the press axis to verify the presence of texture. Intensity measurements of the (006) peak were taken at regular intervals across both the horizontal and the vertical centerlines of the samples, Fig. 2b; (006) rocking curves, *i.e.*, variation of ϕ at the value of 2θ corresponding to the (006) reflection, were also measured. For all samples the count rate was sufficiently large that the scan time was limited by motor speeds, and each rocking curve was generated in about 10 minutes. The peaks were fit to a Lorentzian line shape raised to an arbitrary power, and the width of the peaks were corrected for absorption effects. The absorption generates peak widths that depend on the x-ray energy and sample thickness. The Lorentzian line shape produced a significantly better fit than a Gaussian line shape. The angular half-width of the peak was determined at its half-maximum intensity (HWHM), and the error in the of the peak width is estimated at ±5%.

Fig. 3 displays graphs of both the 2-14-1 (006) peak maximum intensities and HWHM peak breadths for the 42% DU and 70% DU samples. The x-ray beam is no longer on the sample when the (006) peak intensity drops to zero. The (006) reflection for

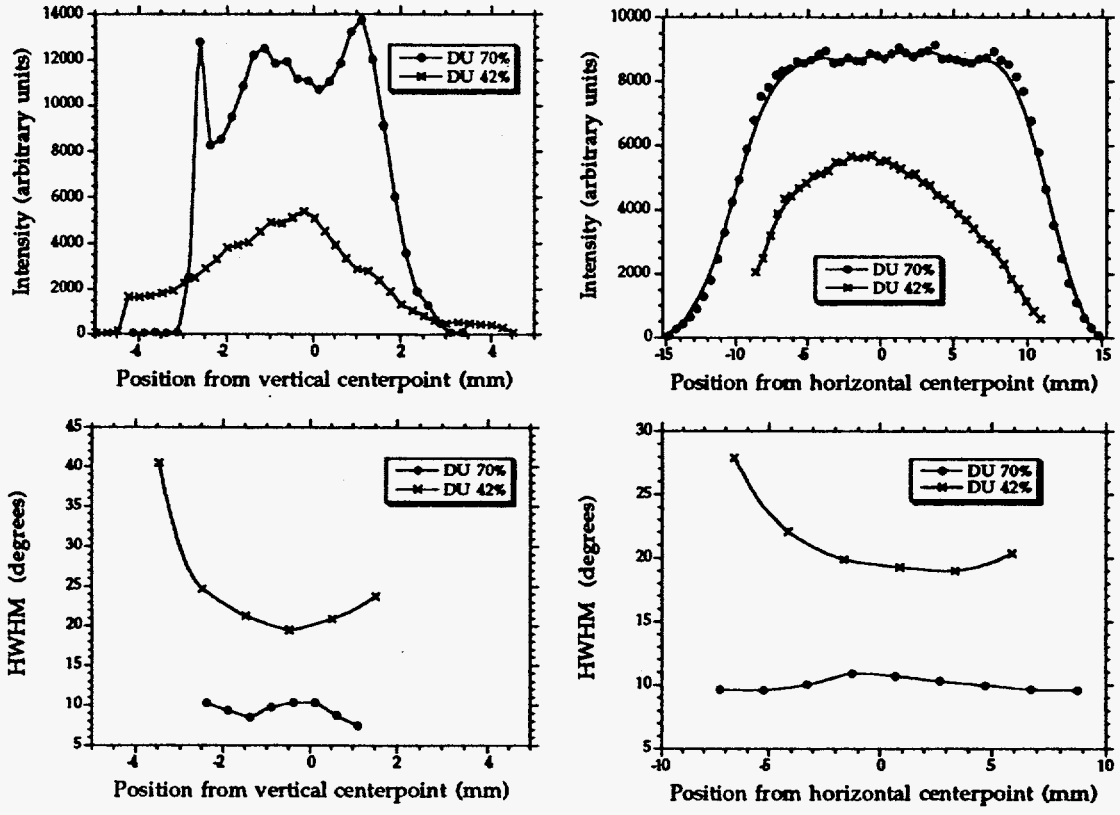

Figure 3. (006) peak maximum intensity and rocking curve width as a function of horizontal and vertical position for samples that have been die-upset to 42% and 70%.

the 0% (isotropic) sample was obscured by the strong Bragg reflections nearby, and thus could not be measured. The rocking curve of an isotropic sample would be flat if absorption effects were absent. When absorption effects are included, an isotropic sample typically has a HWHM of $\approx 28^{\circ}$ for the samples studied here. In all cases the (006) peak intensity varies in the opposite sense from the HWHM as a function of position. Although the peak intensity can vary for a number of reasons that are not related to the breadth of the rocking curve, such as non-uniform sample thickness, the (006) peak intensity is an easily-visible approximate measure of the degree of crystallographic alignment in the volume that the x-ray beam probes. The 42% die-upset sample shows a gentle increase of crystallographic alignment that progresses from the outside of the sample to the center along the diameter, with a maximum in the center of the sample. The variation of alignment in this sample parallel to the press direction is somewhat sharper, demonstrating significantly more alignment in the center of the sample as opposed to the top and the bottom. The spatial variations of crystallite orientation parallel and perpendicular to the press direction found in the 70% DU sample looks distinctly different from the 42% DU. As the distribution is probed across the sample diameter along the centerline it is found that the orientation quickly reaches a constant level in the interior; the HWHM measurements indicate that there may be a slightly increased orientation in the center. The variations of texture measured by rastering the beam parallel to the press direction appears to be bimodal, which may indicate that the top and bottom thirds of the sample deform more severely than the middle third. The data indicate that the development of texture with deformation starts, as expected, in the center of the magnet where the stresses are the greatest. Because the deformation takes place in an oversized die, the sides of the initial compact are initially free to move under the compression, and an elevated strain state develops in the magnet's center region compared to that at the sides. Additionally, temperatures are also higher in the center of the magnet at the start of the deformation cycle. The mechanism responsible for texture development causes a radial progression of alignment from the center toward the periphery. Interestingly, although the rocking curve data indicate that there is a significant difference in the particle alignment between the DU 42% and the DU 70% samples, the bulk demagnetization curves, Fig. 1, do not show a great difference in the bulk magnetic properties. Work is continuing on this characterization[8].

2.2. Paramagnetic Susceptibility Studies

2.2.1. Theoretical Framework

The paramagnetic susceptibility of a material of uniaxial symmetry is a second-rank tensor with two distinct elements: the susceptibilities for magnetic field parallel and perpendicular to the symmetry axis[9]. Thus, in principle, if one has a suitable single crystal with which to establish these two elements, then a measurement of the susceptibility of a textured polycrystal can be used to determine a measure of the degree of texture present. (A discussion of the susceptibility of a random polycrystal may be found in Chapter III, section 4 of ref. 9.) In this presentation the case of temperatures high enough such that a Curie-Weiss-type temperature dependence is observed will be treated, in which case the distinct elements of the susceptibility tensor of each crystallite have the form:

$$\chi_{i=}\frac{C_i}{(T-\theta_i)} \tag{1}$$

where i denotes either the basal (ab) or the axial (c) component. In principle, both the Curie constant C_i and the paramagnetic Curie temperature θ_i depend on the direction of the magnetic field with respect to the crystallite axis. Bowden *et al.*[10] have considered the case of anisotropy in the paramagnetic Curie temperature θ_i that arises from crystal field effects, while Niira and Oguchi[11] have discussed the anisotropy of the Curie constant C_i which can arise from anisotropic g-factors. Anisotropy of C_i can also arise from anisotropic exchange. If it is assumed that both θ_i and C_i are anisotropic, then the transformation properties of second rank tensors[9] show that the paramagnetic susceptibility of an ensemble of independent crystallites, a good approximation to a polycrystal in the Curie-Weiss regime of paramagnetism, even for exchange-coupled two-phase materials, is given by:

$$\chi_p = \frac{C_c}{T-\theta_c} + \langle n^2 \rangle \cdot \left[\frac{C_{ab}}{T-\theta_{ab}} - \frac{C_c}{T-\theta_c} \right] \tag{2}$$

where $\langle n^2 \rangle$ is an ensemble average of the square of the cosine n_i of the angle between the symmetry axis of each crystallite and the applied field (in this case, the direction of pressing during the die-upsetting process). The texture dependence of $\langle n^2 \rangle$ is the key to using the paramagnetic susceptibility as a measure of crystallographic texture: for a random polycrystal $\langle n^2 \rangle = \frac{1}{3}$, while for a perfectly axially-textured polycrystal $\langle n^2 \rangle = 1$. It is convenient to introduce a texture order parameter Σ which lies in the range $0 \le \Sigma \le 1$ for these cases as a measure of the axial texture:

$$\Sigma = \frac{\langle n^2 \rangle - \frac{1}{3}}{1 - \frac{1}{3}} \tag{3}$$

Thus Σ is valid in the range $-1/2 \le \Sigma \le 1$, where $\Sigma=1/2$ describes the isotropic 2d case with all symmetry axes in a plane, $\Sigma=0$ describes the random alignment case, and $\Sigma=1$ is the uniaxially aligned case. In terms of the texture order parameter Σ, the susceptibility of the polycrystal is

$$\chi_p = \frac{1}{3} \cdot \left\{ \frac{2C_{ab}}{T-\theta_{ab}} + \frac{C_c}{T-\theta_c} \right\} + \frac{2\Sigma}{3} \cdot \left\{ \frac{C_c}{T-\theta_c} - \frac{C_{ab}}{T-\theta_{ab}} \right\} \tag{4}$$

If the single crystal parameters C_{ab}, C_c, θ_{ab} and θ_c are known, then a measurement of the polycrystalline susceptibility yields the texture order parameter Σ for the polycrystal. This, however, is not necessarily the case, since processing may alter the values of C_i and θ_i as well as the texture. Thus it is of value to simplify and approximate Eq. 4. The experimental data of Burzo *et al.*[13] and Liu *et al.*[14] show that the deviation of the paramagnetic Curie temperature θ_p from the thermodynamic Curie temperature T_c is small compared with T_c for both polycrystals[13] and single crystals[14]. Furthermore, these data plus our own work show that the anisotropy of θ_p, $\frac{(\theta_c - \theta_{ab})}{T_c}$, is also small. To first order in this anisotropy and in the anisotropy of the Curie constant, $\frac{(C_c - C_{ab})}{C_c}$, Eq. 4 becomes:

$$\chi_p^{-1} \equiv \left(\frac{T}{\theta_p} - 1\right) \cdot \left\{\frac{T_c}{C_c} \cdot \left[1 - \frac{2}{3} \cdot \left(\frac{\Delta C}{C_c} - \frac{\Delta\theta}{T_c}\right) \cdot \Sigma\right]\right\} \qquad (5)$$

where θ_p and T_c are the paramagnetic and thermodynamic Curie temperatures, respectively, of the polycrystal and $\Delta C \equiv C_c - C_{ab}$, $\Delta\theta \equiv \theta_c - \theta_{ab}$. (In the derivation of Eq. 5 it was assumed that the deviation of θ_p from T_c arises from crystal field effects only, and that, following the use of experimental crystal field coefficients of Boltich and Wallace[12] in the theory of Bowden *et al.*[10], $\theta_c > \theta_{ab}$.)

From Eq. 5 we see that a plot of the inverse susceptibility χ_p^{-1} versus the scaled temperature $\frac{T}{\theta_p}$ yields a straight line with a slope that varies linearly with the texture order parameter Σ. The condition that this slope increases with decreasing texture, as is observed experimentally and discussed in Section 2.2.2 below, is simply that $\frac{C_c - C_{ab}}{C_c} > \frac{\theta_c - \theta_{ab}}{T_c}$, *i.e.*, that the fractional anisotropy of the Curie constant be dominant over the fractional anisotropy of the paramagnetic Curie temperature.

Finally, a contact may be made, in an approximate way, between the x-ray determination of texture discussed in Section 2.1 and the texture order parameter Σ which appears in Eq. 5 by using a simple "box distribution" to describe the distribution of misorientation angles between the crystal symmetry axis and the die-upset direction. The box distribution is described as follows: for misorientation angles less than Φ, the distribution of crystal axes is uniform over a solid angle; for those angles greater than Φ, there are no crystals with such misorientation. If the "box distribution" is chosen so as to match its variance with that of the true distribution, the cutoff parameter Φ is approximately 2.7 times the half-width at half-maximum (HWHM) of the rocking curve. The texture order parameter Σ is related to the box-distribution cut-off angle Φ as:

$$\Sigma \equiv \frac{\cos\Phi \sin^2\Phi}{2\cdot[1-\cos\Phi]} \qquad (6)$$

Note that for good textures, with only small deviations from uniaxial alignment, $\Sigma \approx \left[1-\left(\frac{\Phi^2}{2}\right)\right]$, so that small deviations do not affect the paramagnetic susceptibility very much because of the quadratic variation in Φ; this appears to be the case experimentally, as noted in section 2.2.2 below.

2.2.2. Experimental Procedures and Results:

Magnetic measurements were made on a series of samples with nominally the same composition but were processed in different manners. The composition and processing details of the samples are included in Table I; for comparison purposes the susceptibility data from single-phase $Nd_2Fe_{14}B$ powder[13] and a single $Nd_2Fe_{14}B$ crystal[14] are also included. The experimental samples were machined down to the appropriate dimensions to fit inside quartz capillary tubes that were evacuated to a base pressure of 5.6×10^{-5} torr and sealed with Zr turnings to avoid oxidation during measurement. Prior to each hysteresis loop measurement the magnets were brought to temperature and then saturated in an applied field of +5.0 T. The resultant hysteresis loops were corrected for demagnetization using a method previously described[15].

Table I: Descriptions of $Nd_2Fe_{14}B$-based samples:

Processing	*Bulk Composition*
Die-upset (MQ-3)	$Nd_{13.75}Fe_{80.25}B_6$
Sintered	$Nd_{15}Fe_{78.5}B_{6.5}$
Hot-pressed (MQ-2)	$Nd_{13.75}Fe_{80.25}B_6$

In every case the magnets were confirmed to consist mainly of $Nd_2Fe_{14}B$ with a small amount of an unknown ferromagnetic phase with a Curie temperature T_c in the vicinity of 950 °C[16]. The amount of unknown ferromagnetic material is on the order of 0.1 vol%. Additionally, room-temperature saturation magnetization measurements indicate that the sintered sample contains only 86% of the $Nd_2Fe_{14}B$ phase, the remainder presumably being the 1-4-4 phase; the slope of the paramagnetic signal was adjusted for this deficiency. The paramagnetic signal from the 2-14-1 matrix phase and the ferromagnetic signal of the unknown phase were separated from one another[16]. Fig. 4 shows the inverse of the susceptibility of the paramagnetic portion of the signal graphed as a function of reduced temperature, T/θ_P, where θ_P was determined experimentally as the linear extrapolation of the inverse susceptibility to the temperature axis. The legend of Fig. 4 includes the determined paramagnetic Curie temperatures. Included in Fig 4 are the susceptibilities of the data taken from the literature for the $Nd_2Fe_{14}B$ in both single crystal and powder form. The crystal was measured along the easy-axis *c*-direction. It should be noted that Liu *et al.* determined the single crystal to possess a Curie temperature of 574 K, approximately 20 degrees lower than the accepted literature values of 595 K - 600 K[17]. In accordance with the formalism outlined in Section 2.2.1 above, the experimental inverse susceptibilities *vs.* reduced tem-

perature curves exhibit slopes which increase with decreasing sample alignment. The inverse susceptibility slopes increase from the single crystal and MQ-3 sample to the sintered sample and are highest for the powder and hot-pressed samples. It is reassuring that the

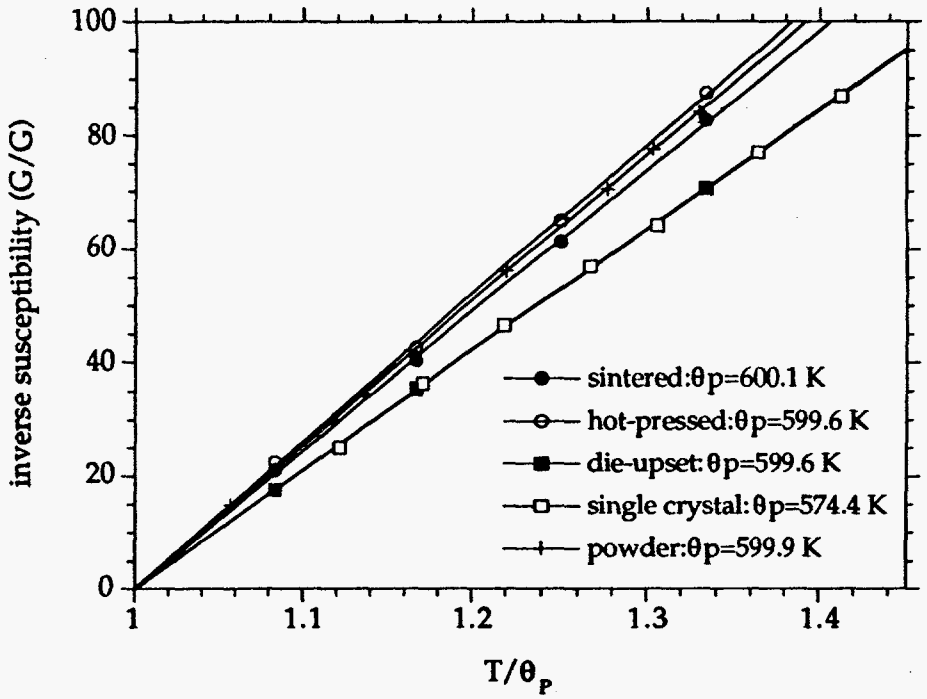

Figure 4. Inverse susceptibilities of $Nd_2Fe_{14}B$ magnetic materials in various processed forms.

two isotropic samples, the powder the hot-pressed samples, both exhibit very similar slopes. However, it is not expected that the single crystal and the MQ-3 sample would have exactly the same slope; this result may be explained by the observation (mentioned in Section 2.2.1) that the slope of the inverse susceptibility curve is not sensitive to small misorientation angles.

3. Summary

We have briefly outlined here the methodology and underlying rationale for two new techniques that may be used to probe the crystallographic texture distribution in a magnetic material. These techniques, while preliminary, may prove to be useful in circumstances that preclude the use of the more standard determinations of magnetic remanence, B_r, such as in the case of novel exchange-spring magnets. Data consisting of selected peak intensities and rocking curve half-widths obtained from transmission x-ray diffraction provide information concerning the development of texture in two melt-quenched and deformed magnets based on $Nd_2Fe_{14}B$. As expected, it is found that the alignment is initiated in the center of the magnet, where the stress is the greatest, and moves out radially with increasing pressure.

The trend of the inverse paramagnetic susceptibility *vs.* temperature data collected from a selection of $Nd_2Fe_{14}B$-based magnetic materials fabricated by different methods

agrees with that predicted from a simple linearization of the Curie-Weiss law for textured polycrystals that has been rewritten to take into account both anisotropic paramagnetic Curie temperatures and anisotropic Curie constants. While this method does provide qualitative information concerning the relative crystallographic alignment of magnet samples, it needs calibration to obtain an explicit value for the texture order parameter. In principle, it is possible to derive an explicit order parameter and to use it to obtain a quantitative particle misorientation distribution.

4. Acknowledgments

The authors would like to thank F. Pourarian of the Carnegie Mellon Research Institute for supplying samples and J.-Y. Wang for help with computer graphics. This research was performed under the auspices of the U.S. Department of Energy, Division of Materials Sciences, Office of Basic Energy Sciences under Contract No. DE-AC02-76CH00016. Research was carried out in part at the National Synchrotron Light Source, Brookhaven National Laboratory, which is supported by the U.S. Department of Energy, Division of Materials Science and Division of Chemical Sciences.

5. References

1. G. Asti, F. Bolzoni and L. Pareti, *J. Magn. Magn. Mater.* **83** (1990) 270; K. Elk and R. Hermann, *J. Magn. Magn. Mater.* **128** (1993) 138.
2. W. C. Chang, T. B. Wu and K. S. Liu, *J. Appl. Phys.* **63** (8) (1988) 3531; G. P. Meisner and E. G. Brewer, *J. Appl. Phys.* **72** (7) (1992) 2659.
3. R. K. Mishra, *J. Appl. Phys.* **62** (3) (1987) 967; L. Li, D. E. Luzzi and C. D. Graham Jr., *J. Appl. Phys.* **70** (10) (1991) 6459.
4. S. R. Trout and C. D. Graham Jr., *IEEE Trans. Magn.* **MAG-12** (1976) 1015.
5. R. Skomski, *J. Appl. Phys.* **76** (10) (1994) 7059.
6. K. Elk, L. Hahn and R. Scholl, *J. Magn. Magn. Mater.* **72** (1988) 335.
7. E. C. Stoner and E. P. Wohlfarth, *Philos. Trans. Roy. Soc. London* A **240** 599 (1948).
8. L. H. Lewis, D. O. Welch, T. R. Thurston and V. Panchanathan, in preparation.
9. J. F. Nye, *Physical Properties of Crystals* (Oxford, Clarendon Press, London, 1957).
10. G. J. Bowden, D. St. P. Bunbury and M. A. H. McCausland, *J. Phys. C: Solid St. Phys.* **4** (1971) 1840.
11. K. Niira and T. Oguchi, *Prog. Theo. Phys.* **11** (1954) 425.
12. E. B. Boltich and W. E. Wallace, *Solid State Commun.* **55** (1985) 529.
13. E. Burzo, E. Oswald, M.-Q. Huang, E. Boltich and W. E. Wallace, *J. Appl. Phys.* **57** (1) (1985) 4109.
14. Y. Liu, L. Mei, H. Chen and F. Chen, *Chinese Phys. Lett.* **4** (11) (1987) 513.
15. L. H. Lewis, Y. Zhu and D. O. Welch, *J. Appl. Phys.* **76** (1994) 6235.
16. L. H. Lewis, D. O. Welch and F. Pourarian, *J. Appl. Phys.*, in press.
17. J. Herbst, *Rev. Mod. Phys.* **63** (4) (1991) 819.